



POLARON ON HARMONIC LATTICE IN ELECTRIC FIELD GENERATION OF COHERENT OSCILLATIONS

T. Yu. Astakhova^{[a]*} and G. A. Vinogradov^[a]

Keywords: Polaron, charge transfer, electron-lattice interaction, electron-phonon interaction, SSH.

The dynamics of a polaron on a one-dimensional harmonic lattice in an applied constant electric field has been considered. The calculations were performed with parameters close to those of polyacetylene and DNA. The polaron in a constant field goes to a stationary state, characterized by a constant profile and velocity. In this case, the energy got by the polaron from the electric field is transformed into longitudinal coherent lattice vibrations. For several thousand lattice sites, these oscillations have constant frequency and wave number, and these values depend weakly on the electric field.

* Corresponding Authors

Fax: +7(495) 9390838, +7(916) 1360239

E-Mail: astakhova@deom.chph.ras.ru

[a] Emanuel Institute of Biochemical Physics, Russian Academy of Sciences, Moscow, Russian Federation
119334, 4 Kosygina st, Moscow, Russia

INTRODUCTION

Presently, nano-sized electronic devices is widely used in various fields¹⁻¹⁰ and their uses have been reviewed also.^{11,12} It is supposed that polarons are charge carriers in nonmetallic systems. Really, a minimum energy state of a charged elastic lattice with electron-phonon interaction corresponds typically to polaron formation.

Historically, polaron studies on one-dimensional lattices started with the modelling of a charged soliton in polyacetylene (PA).¹³⁻¹⁷ First, an analysis of the effect of an external electric field on a charged soliton was done.¹⁸ Later, the study of polaron in an external electric field was conducted.¹⁹

The energy and charge transfer in biological macromolecules, such as DNA and polypeptides, has been intensively investigated for a long time. The conduction mechanism picture in such systems evolved from the Marcus theory²⁰ to the tunneling²¹ and hopping mechanism.²² Further, the polaron mechanism of conductivity was proposed. Conwell and coworkers first applied polaron paradigm to DNA.²³⁻²⁶ Later, various models and approximations of the polaron charge transport in DNA were developed.²⁷⁻³⁷

One of the most common methods for calculating the electronic structure and transport properties is the tight-binding approximation (TBA),^{38,39} otherwise called the Huckel method. In this approximation, the wave function is represented as a linear combination of localized states. In the particular case of molecular systems, this is a linear combination of atomic orbitals. The most popular method for describing the electron-phonon interaction is the Su-Schrieffer-Heeger (SSH) approximation, first used to describe charged solitons in PA.^{16,17}

The SSH model for PA includes minimum parameters necessary for polaron description. Namely, σ bonding is taken into account through harmonic interaction between nearest units (representing CH groups) of one dimensional lattice, and π electrons are treated in TBA. The units displacements are measured from positions of undimerized chain and dimerization is taken into account by the alternation of displacements sign. Another way to include dimerization is Brazovskii-Kirova symmetry breaking terms.^{40,41} Subsequently, the SSH model became widely used for description not only for simple conjugated polymers but more complicated systems, for example, DNA,^{23-26,42-44} polypyrrole⁴⁵ and paraphenylene polymers (PPP).⁴⁶ The electron-phonon coupling can be taken into account in a slightly different way also, as in the case of Frohlich or Holstein polarons⁵²⁻⁵⁵ or in Davydov-Scott model.⁵⁷ However, in all models the general polaron behaviour is similar. Nonlinearity has also been included in dependence of the hopping integral on the distance between chain units.⁵⁸ Further, the polaron models were complicated by addition spin and Coulomb interactions for bipolarons,^{40,46,47} thermal^{48,59-61} and disorder^{62,63} effects, and impurities.^{64,65} Two-dimensional lattices including interchain interactions were also considered.^{49-51,55,56} Higher order tight binding SSH model has been developed for DNA charge transport.⁷⁰

Polarons as charge carriers can be accelerated under an external electric field.^{19,68-70} The charge motion in semiconductors and insulators was first considered by Feynman.⁷¹ It was found that the polaron transforms the energy of interaction with the electric field into vibrational energy. For Al₂O₃ the transferred energy is ~0.025 eV per 1 Å.

In the SSH model, the electric field can be taken into account either by vector potential or by a term which explicitly describes the voltage drop between neighbouring sites.^{68,80} These descriptions are equivalent and interrelated through a gauge transformation.

It was found that polaron achieves maximum velocity in electric field. In simple SSH model without dimerization maximum polaron velocity is always less than the sound velocity. If dimerization is taken into account supersonic velocities can be achieved when optical mode is excited.^{66,73} There is maximum electric field which destroys polaron.⁷²

The reported value of the critical electric field in PA widely varies in the literature (10 mV/Å,^{47,74,75} 4 mV/ Å,⁵⁰ 0.54 mV/Å⁴⁶ and 1.6 mV/Å⁷⁶ in polyparaphenylene). Critical field values for a number of inorganic polymers have reported⁷² e.g., 3.9 mV/Å for PA, 1.3 mV/Å for polystannane, 1.3 mV/Å for polygermane, and 1.3 mV/Å for polysilane. In some papers the lattice vibrations following moving polaron in electric field are reported.^{77,78} Above the critical field, the dissociated polaron propagates in the form of a free electron and performs spatial Bloch oscillations.⁶⁷ On the other hand, Bloch oscillations in the electric field can generator polarons in a 1D crystal.⁷⁹ Theoretical investigation of the simple SSH model with one electron on the harmonic lattice has been reported by Basko and Conwell.⁸⁰ Here, analytical dependence of the polaron velocity versus applied electric field has been presented. The critical electric field value is also estimated.

In present study, the polaron dynamics on harmonic lattice in an electric field is thoroughly investigated numerically in the framework of SSH model. A harmonic lattice with parameter close to polyacetylene and DNA has been considered. A weak logarithmic dependence of the stationary polaron velocity on the value of applied electric field is found. Mechanisms of energy transfer from a moving polaron to a lattice are discussed. The parameters of coherent vibrations generated by polaron moving in external electric field are investigated. Critical field for PA and DNA parameters are estimated. We found good agreement with the reported theoretical prediction.⁸⁰

MODEL

We use the following generally accepted Hamiltonian,⁶⁸ where eqn. (2) describes the dynamics of regular harmonic lattice. Here, x_j and v_j are the deviation of the j -th particle from the equilibrium and its velocity, K is the rigidity, M is the particle mass.

$$H = H_{\text{lat}} + E_{\text{el}} \quad (1)$$

$$H_{\text{lat}} = \frac{K}{2} \sum_j (x_{j+1} - x_j)^2 + \frac{M}{2} \sum_j v_j^2 \quad (2)$$

The second, quantum term in eqn. (1) is the electronic part of the total Hamiltonian. It is written in the TBA approximation in an external constant electric field as eqn. (3).

$$H_{\text{el}} = - \sum_j [t_0 - \chi(x_{j+1} - x_j)] [\exp(i\gamma A) c_j^+ c_{j+1} + \text{c. c.}] \quad (3)$$

Here, the electron-phonon interaction (EPI) is described in SSH approximation, t_0 is the equilibrium hopping integral, χ is the EPI parameter, and c_j^+ / c_j are the creation/annihilation operators for the electron at the site j , and c.c. stands for complex conjugation.

As a rule, dimensionless quantities were used. For non-dimensionalization, four independent parameters should be chosen. It is convenient to choose M , K , t_0 , and the electron charge e . The numerical values⁷⁰ of these parameters for

DNA are $M = 4.35 \times 10^{-25}$ kg, $K = 13.6$ kg s⁻², $t_0 = 4.8 \times 10^{-20}$ kg m² s⁻², $e = 1.6 \times 10^{-19}$ C. At the non-dimensionalization, the numerical values of these parameters are taken to be unity. After that, all other parameters can be dimensionless. The dimensionless unit length is defined as $[[L]] = (t_0/K)^{1/2}$, and it corresponds to 0.59 Å. Similarly, the dimensionless time unit is defined as $[[t]] = (M/K)^{1/2}$, which corresponds to 0.18 ps. The dimensionless unit of energy is 0.3 eV. Dimensionless values of other parameters of the Hamiltonian are defined similarly: $\hbar \approx 10^{-2}$ and $\chi \approx 1.2$.

Since the numerical values of the parameters M , K and t_0 in PA differ from those in DNA,⁶⁷ the corresponding dimensionless parameters were renormalized. The length, time, and energy units are $[[L]] = 0.35$ Å, $[[t]] = 8$ fs, $[[E]] = 2.5$ eV, respectively, and the EPI parameter $\chi \approx 0.4$. Note that $\chi = 0.4$ is maximum value for which the continuum approximation works well. So, exact expressions for the polaron shape and the wave function are available.^{81,82}

The external electric field is taken into account by a factor $\exp(i\gamma A)$, where $\gamma = ea/\hbar c$ and e is the electron charge, a is the lattice constant, c is the light speed, \hbar is Dirac's constant. The relation between the vector potential A and electric field E is $E = -1/c dA/dt$. It is convenient to write the exponential term as $\exp(-iBt)$, where $B = eEa/\hbar$. Below, we use B and call it an electric field parameter. For DNA and PA, the dimensionless value $B = 1$ corresponds to $E \approx 1.1 \times 10^7$ V m⁻¹ and $E \approx 6.8 \times 10^8$ V/m, respectively.

After non-dimensionalization we get the following evolutionary equations for both classical and quantum degrees of freedom where $F \equiv \exp(iBt)$.

$$\begin{aligned} \ddot{x}_j = & -(2x_j - x_{j+1} - x_{j-1}) \\ & + \chi \left[F \psi_j^* \psi_{j-1} - F^* \psi_{j-1}^* \psi_j + F \psi_{j+1}^* \psi_j \right. \\ & \left. + F^* \psi_j^* \psi_{j+1} \right] \end{aligned} \quad (4)$$

$$\dot{\psi}_j = -\frac{i}{\hbar} \{ [-1 + \chi(x_{j+1} - x_j)] F \psi_{j+1} + [-1 + \chi(x_j - x_{j-1})] F^* \psi_{j-1} \} \quad (5)$$

The time evolution of a polaron in electric field is obtained by numerical integration of eqns. (4) and (5) with free boundary conditions. The integration step Δt is determined by the most "fast" quantum dynamics for the wave function, and therefore $\Delta t = 10^{-4}$ is chosen.

POLARON IN ELECTRIC FIELD

The polaron on a harmonic lattice in an electric field reaches a steady state with a constant velocity and an unchanged profile of the polaron.⁸⁰ However, the stationary state setting time and the final polaron parameters depend strongly on the initial conditions.⁶⁹ Polaron evolution is also sensitive to the method of electric field switching. If the

switching time is small, a part of the electron density can decouple from the lattice deformation and the polaron can fail.

Initial conditions

Parameters of the polaron on a harmonic lattice without an electric field (velocity, amplitude and width) are uniquely related, and the choice, for example, of the velocity determines the polaron profile.

For small EPI parameter ($\chi \leq 0.4$) the continuum approximation is valid and analytical relations⁸³ for relative displacements of neighbouring particles $q_j \equiv (x_j - x_{j-1})$ and the wave function $\psi_j(t)$ are available (eqn. 6), where A and D are amplitudes of relative particles displacements and wave function, respectively, $1/d$ is a polaron width, j_0 is the initial polaron centre, v is the polaron velocity.

$$q_j = -\frac{A}{\cosh^2[d(j-j_0-v_0t)]},$$

$$\psi_j = \frac{B}{\cosh[d(j-j_0-v_0t)]} \quad (6)$$

The following three equations relate polaron parameters.

$$d = \sqrt{\chi A}, v_0 = \left[1 - \sqrt{\chi^3/A}\right]^{1/2} \text{ and}$$

$$B = \sqrt{d/2} \quad (7)$$

According to eqn. (7), polaron can be determined by any one parameter. It is convenient to choose the velocity v as a free parameter.

The polaron velocity on a harmonic lattice varies from zero to the nearly sound velocity, v_{snd} . Therefore, when modelling a polaron evolution in an electric field, the initial polaron velocity can be chosen in the range $0 < v_0 < v_{\text{snd}}$. Another simulation parameter is the electric field strength (dimensionless parameter B in (eqns. 4 and 5) and the method of the field switching-on (Figure 1).

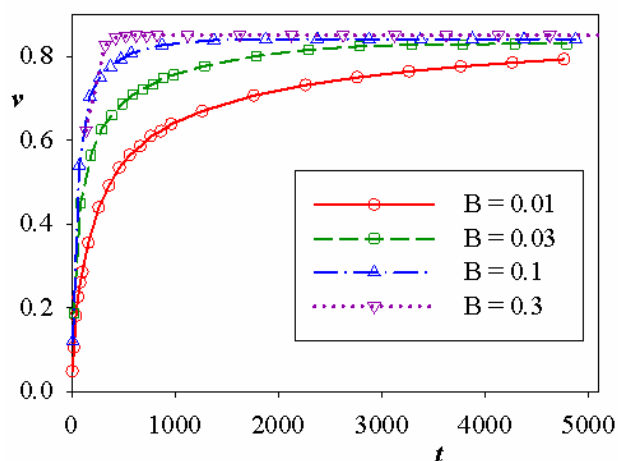


Figure 1. The dependence of polaron velocity v on time t for different values of electric field parameter B . Initial polaron velocity is zero. The field switching-on rate is $1/1250$, $\chi = 0.4$.

Let us consider the setting of a stationary polaron velocity depending on the electric field for initially standing polaron. The time dependence of polaron velocity for different B is shown in figure 1. Here, $\chi = 0.4$, which corresponds to the PA. In all cases, the field grows linearly ($B = ct$) for a period of time τ up to the maximum value B_{max} , and $c = B_{\text{max}}/\tau = 1/1250$. In figure 1, all dependencies start at $t = \tau$, when the field reaches its maximum value. At small electric field, the polaron accelerates further after reaching B_{max} as it doesn't reach the maximum possible velocity. Hereafter, the polaron velocity is measured in the sound velocity.

For $\chi = 0.4$, the stationary dimensionless polaron velocity $v_{\text{st}} \approx 0.86$, which is $\approx 1.3 \times 10^4 \text{ m s}^{-1}$ in dimensional units. The dependence of the steady-state polaron velocity on the applied electric field is considered in more detail below. Polaron behaviour similar, to that in Figure 1, is also observed for $\chi = 1.2$, which corresponds to the DNA. Here, however, the stationary dimensionless velocity is less and $v_{\text{st}} \approx 0.6$, which corresponds to $\approx 1.1 \times 10^3 \text{ m/s}$.

In the examples considered above, the total density of the wave function is localized on the polaron and is equal to the total charge of the electron. However, for some initial conditions, a part of the electron density can partially decouple from the lattice deformation,⁶⁷ and the polaron, being stable, carries a partial charge less than unity. The decoupled part of the wave function density is randomly distributed along the lattice (Figure 2).

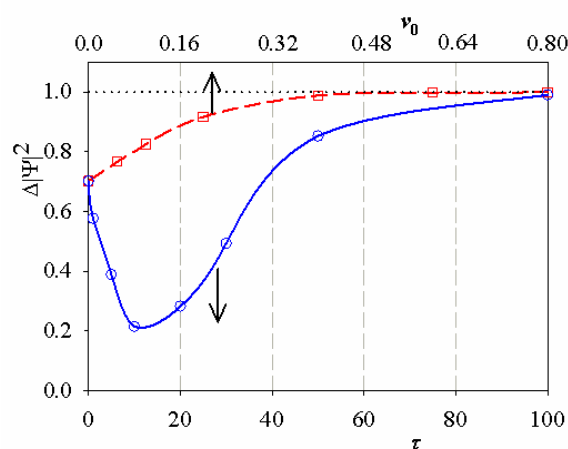


Figure 2. A fraction of electron density localized on the polaron $\Delta|\Psi|^2$ as function of switching-on time τ (solid line, open circles); $\Delta|\Psi|^2$ vs initial polaron velocity v_0 (dashed line, open squares) at instant field switching-on; $\chi = 0.4$.

If at first the field increases linearly ($B = B_{\text{max}}/\tau$ for $t \leq \tau$ and $B = B_{\text{max}}$ for $t > \tau$), then the fraction of the electron density $\Delta|\Psi|^2$ left at the polaron depends on τ nonmonotonically. The result is shown in figure 2 (solid curve and circles). Here, $B_{\text{max}} = 0.08$, $\chi = 0.4$, and the initial polaron velocity is zero. One can see that when the electric field is slowly switched on ($\tau > 100$), the polaron keeps practically 100 % of the wave function density. Another example of non-conservation of the wave function density is shown in the same figure (dashed lines and squares). Here the field is switched on instantly, but the initial polaron velocity changes from zero to $v_0 = 0.8$. Even if a part of the

charge leaves the polaron, it remains stable. But in this case its amplitude decreases, and the width increases because of the renormalization of the wave function on the polaron. Similar polaron behavior is observed for $\chi = 1.2$. However, in this case the polaron is more "compact" (it has a smaller width and a larger amplitude), the wave function is better attached to the polaron, and the polaron itself is more stable to the variation of the initial conditions.

Thus, figure 2 demonstrates the closer the initial conditions correspond to the stationary state of the polaron, the faster and more "confident" the polaron reaches this stationary, while maintaining the complete norm of the wave function. In all numerical simulation, only such initial conditions are used below, which provide at least 99 % localization of the wave function density at the polaron.

Stationary polaron velocity

Numerical simulations reveal that the relations between polaron parameters (amplitude, velocity, width) do not depend on the presence of the electric field. That is, the field initially only accelerates the polaron, and after that it moves at a constant velocity as if without the field. The influence of the electric field is discussed in more detail below.

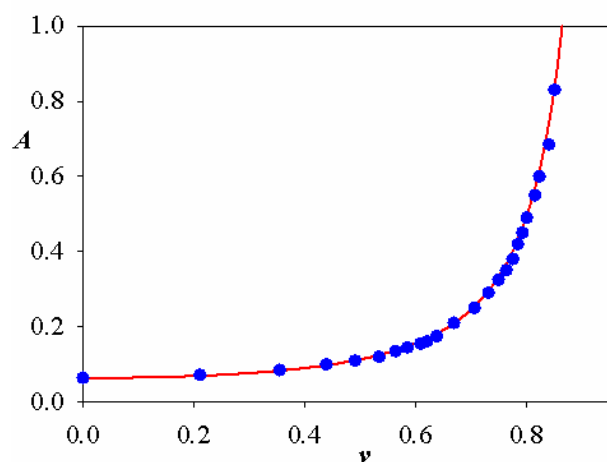


Figure 3. Amplitude of relative displacements A vs polaron velocity v without electric field (solid line is analytics⁸³) and in electric field (circles, numerical simulation); $\chi = 0.4$

Figure 3 shows the relation between the amplitude and the velocity of the polaron in the electric field and without the field for the EPI parameter $\chi = 0.4$. Circles in figure 3 corresponds to data in Figure 1 when the polaron accelerates in electric field of different values. For larger values of χ , e.g. $\chi = 1.2$, the continual approximation is not applicable because the corresponding polaron is narrow. However, as the polaron with $\chi = 1.2$ is much more stable in the electric field and quickly reaches the stationary state, the initial values of the polaron parameters are less significant. And it is reasonable to set initial conditions according to eqn. (6), choosing polaron parameters so that at least 99 % of the wave function density is localized at the polaron during the further evolution. In this case the wave function is the lowest-energy eigenfunction at the Hamiltonian diagonalization (eqn. 3).

The dependence of the steady-state velocity on the field strength B is weakly logarithmic. Figure 4 demonstrates less

than 10 % difference in stationary polaron velocities within four orders of magnitude of the field strength. Therefore, in polyacetylene and DNA, the stationary polaron velocity slightly depends on the applied electric field. The small polaron velocity in very low field can be explained by the fact that the polaron has not yet reached a stationary state during the numerical simulation ($t \leq 10000$). Note, the dependences in Figure 4 are in good agreement with the dependences of the polaron velocity on the applied field.⁸⁰

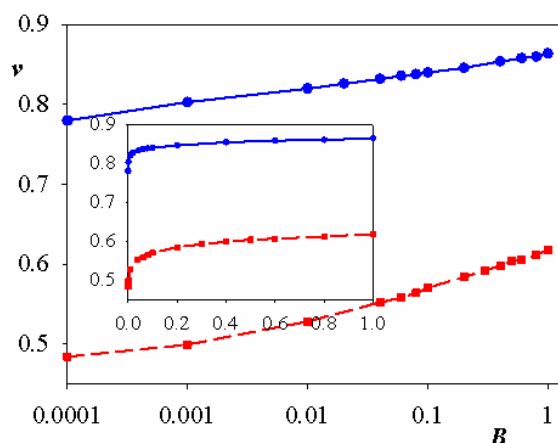


Figure 4. Stationary polaron velocity v vs electric field parameter B for $\chi = 1.2$ (dashed line and squares) and $\chi = 0.4$ (solid line and circles). The dimensionless velocity is measured in units of sound velocities. The inset shows dependencies in linear coordinates.

Generation of longitudinal coherent vibrations

The energy transferred from the electric field to the polaron, in general, can be used in several ways. First, this energy can be spent on accelerating the polaron and, accordingly, on increasing its kinetic energy. Secondly, energy can provide growth of potential energy due to a change in the polaron shape with an increase of the amplitude and a decrease of the width. Correspondingly, the electron energy changes due to the electron-phonon interaction. Finally, some of the energy can be transferred to lattice vibrations.

After the polaron reached a stationary state, the polaron continues to receive energy due to the interaction of the charge with the electric field. The constant power of this interaction is $p = f v_{st}$, where $f = eE$ (e is the polaron charge, E is the electric field strength, v_{st} is the stationary polaron velocity). In this case, the total energy of the "polaron + external field" system grows linearly with time. Since the polaron self-energy does not change, all the power consumed is converted only into lattice vibrational energy. Thus, the polaron velocity is determined by the balance of energies: the energy gained by the polaron in the electric field should be equal to the energy dissipated into the lattice.

The two top panels of figure 5 show snapshots of particles relative displacements $q_j \equiv (x_{j+1} - x_j)$ for $\chi = 0.4$ (left top panel) and $\chi = 1.2$ (right top panel). The polaron moves from left to right and is located on right ends. The lattice oscillations following the moving polaron can be divided into two regions. In region a, the oscillations are irregular

because they are generated during the field switching-on period. Region b can cover several thousand lattice periods and represents coherent oscillations. (Figure 6.)

The time dependence of chosen bond $q_{500} = x_{501} - x_{500}$ oscillations is shown in Figure 6. Polaron passes the bond at

$t = 762$. After this, the bond oscillates with constant frequency and amplitude. The apparent amplitude modulation is due to the incommensurability of the oscillations period and the period of the particle displacement measurement, as illustrated in the inset to the figure.

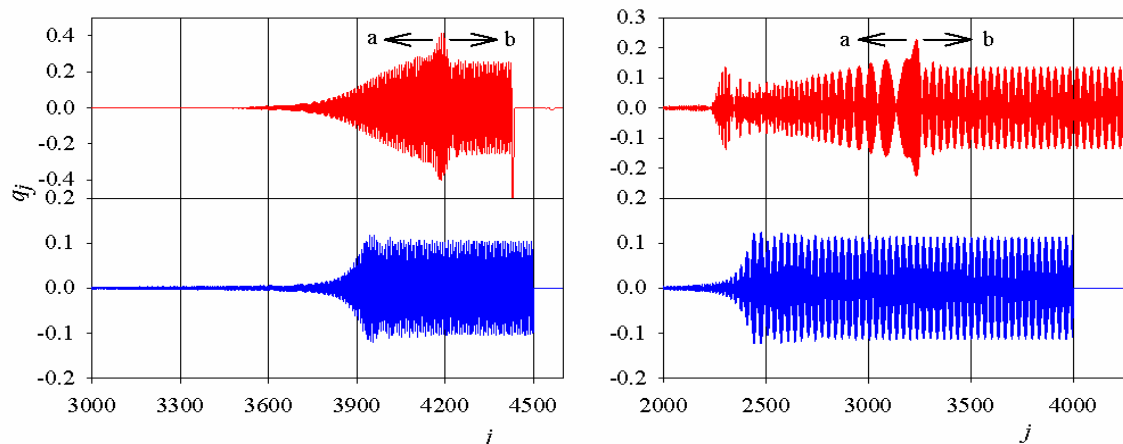


Figure 5. Snapshots of the relative displacements q_j at the time t . Upper row: polaron on the harmonic lattice in electric field. The left upper panel: $\chi = 0.4$, $\nu_0 = 0.8$, $B = 0.1$, $t = 2250$. The right upper panel: $\chi = 1.2$, $\nu_0 = 0.65$, $B = 1.0$, $t = 2825$. In both cases, the polaron was initially located at $j_0 = 2500$ and the field switching-on rate is $c = 1/1250$. Polarons are centered at $j = 4380$ and $j = 4420$ in the left and right panels, respectively. Lower row: the "demon" model (see Section 3.5). The lower left panel: $\nu_d = 0.862$, $t = 2320$. The right lower panel $\nu_d = 0.617$, $t = 2430$. In both cases, the excitation is initially localized at $j_0 = 2500$.

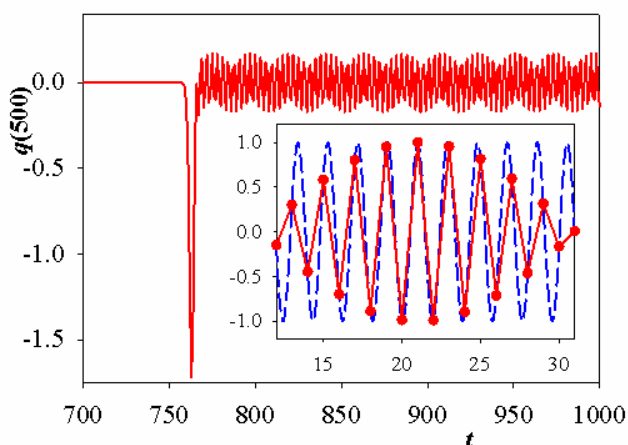


Figure 6. Relative displacement q_{500} vs time, $\chi = 1.2$. The inset illustrates the incommensurability of the true oscillations period (dashed line) and the period of numerical calculation (solid line).

Both space and time Fourier spectra have one peak corresponding to the wave number k (the wavelength $\lambda = 2\pi/k$), and frequency ω of the generated oscillations, respectively. Thus, moving polaron generates stable coherent oscillations described by the equation $q_j = C \sin(kj + \omega t + \varphi)$, where φ is the phase. The values of k and ω are determined by the polaron velocity and the amplitude is determined by the applied field strength, which is in agreement with the reported value.⁸⁰ The dependence of k and ω on polaron velocity is discussed below.

Spectral characteristics of generated coherent vibrations

In the previous section, it was shown that the generated vibrations have definite values of k and ω . Because of the

fact that the field parameter B is uniquely related with the stationary polaron velocity (Figure 3), it is convenient to depict the spectral characteristics k and ω through the stationary polaron velocity v . These dependences are shown in figure 7.

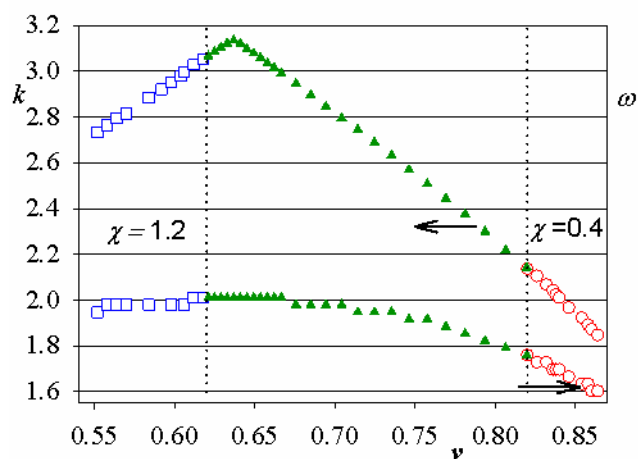


Figure 7. Dependences of the wave number k (upper curve and symbols) and the frequency ω (lower curve and symbols) on the polaron velocity for $\chi = 1.2$ (empty squares) and $\chi = 0.4$ (empty circles) and on the "demon" velocity (filled triangles). Symbols for the wave number refer to the left axis, and symbols for the frequency refer to the right axis.

It is seen that the wave numbers k of the oscillations generated by the polaron do not vary very much, $1.8 \leq k \leq 2.1$ for $\chi = 0.4$ in the velocity range $0.82 \leq v \leq 0.86$ (empty circles in Figure 7), and $2.7 \leq k \leq 3.1$

for $\chi=1.2$ in the velocity range $0.55 \leq v \leq 0.62$ (empty squares in Figure 7). The character of k versus v dependences is different. The wave number increases with increasing speed for $\chi = 1.2$ (empty squares), and decreases for $\chi = 0.4$ (empty circles). The wavelength of the shortest-wave "optical" mode on the harmonic lattice is $\lambda = 2$ in the lattice constants, which corresponds to $k = \pi$. This means that for $\chi = 1.2$ the polaron excites the shortest-wave mode with $\lambda \approx 2.2$. For $\chi = 0.4$, the wavelength of the excited oscillations is slightly larger and $\lambda \approx 3.1$.

The oscillations frequencies are also not very different. The steps-like dependence of ω in Figure 7 is due to the finite value of the integration step. The decrease of the step increases the smoothness of the dependence of ω vs v . In dimensional units, the oscillation frequency is $\approx 2 \times 10^{12}$ Hz at the polaron velocity $v = 0.57$ ($\chi = 1.2$, DNA), and the frequency is $\approx 3 \times 10^{13}$ Hz at the polaron velocity $v = 0.86$ ($\chi = 0.4$, PA).

It was shown⁸⁰ that the wave number k depends on the polaron velocity v and it is determined by the following equation (mod 2π), where v_{snd} is the sound velocity and the frequency is determined by the dispersion equation

$$vk = v_{\text{snd}} \sin(k/2) \quad (8)$$

$$\omega_k = v_{\text{snd}} |\sin(k/2)| \quad (9)$$

Our results are in good agreement with eqns. (8) and (9). Indeed, for $v = 0.8$ and $v = 0.65$ these equations give $k \approx 2.3$, $\omega \approx 1.8$ and $k \approx 3.1$, $\omega \approx 2.0$, respectively. These points fit well in figure 7.

"Demon" Model

As shown above, the moving polaron generates coherent vibrations, and the wave number and the frequency of these vibrations are determined by the applied field (or the polaron velocity). One can say that the polaron is an effective "generator" of stable coherent lattice vibrations, and thousands of lattice sites can participate in these oscillations.

The polaron velocities fall in a narrow range of values ($0.56 \leq v \leq 0.62$ and $0.82 \leq v \leq 0.86$ for DNA and PA, respectively). It is a question, whether generation of such oscillations is possible in some other way than by localized moving compression of special shape. If possible, what are the spectral characteristics of these oscillations over a wider range of velocities of the generating source, and what should be the profile of the generative force.

In light of these questions, eqn. (8) deserves special attention. The fact is that eqn. (4) can be rewritten as $d^2x_j/dt^2 = - (2x_j - x_{j+1} - x_{j-1}) + f_j(t)$, where $f_j(t)$ is a generic force. The force has a profile of a moving impulse, while the profile itself can be of arbitrary shape. In this case, the wave number is determined from the eqn. (8), and the frequency from the dispersion law (eqn. 9).

We propose a simple model called "demon". This is a dynamic model of the compression moving on harmonic lattice in the absence of EPI. The compression has a step-like shape with a width of one lattice period. The power

transferred to the lattice is constant in time and depends on the deformation value. In this model, the demon velocity can vary within $0 < v_d < 1$, which is out of the limits of polaron velocities for two EPI parameters under consideration. We consider the "demon" velocity varying in the range $0.55 \leq v_d \leq 0.9$.

Two lower panels of figure 5 show snapshots of the relative displacements in the harmonic lattice with moving "demon". Comparison of upper and lower panels demonstrates that the oscillations generated by "demon" are very similar to those generated by polaron moving with the same velocity.

Analysis of the spectral characteristics of the generated oscillations shows that the "demon" and the polaron moving with the same velocity excite oscillations with the same wave numbers and frequencies. In figure 7, the frequency and the wave number in the "demon" model are shown by filled triangles. It is seen that in the ranges of polaron velocities, the dependencies for the "demon" model and for polaron in electric field completely coincide. In this case, the wave numbers obey eqn. (8), and the frequencies are calculated from eqn. (9).

Eqn. (8) has a simple physical meaning. For all values of polaron velocity, the equation has one solution which is in the range $0 \leq k \leq 2\pi$, and this solution corresponds to the wave with phase velocity equal to the velocity of the generating source ($v_{\text{phase}} = \omega/k$). It is obvious from combination of eqns. (8) and (9). For small velocities ($v \leq 0.13$), eqn. (8) has more than one solutions. For example, for $v = 0.1$ there are three solutions, $k_1 = 5.705$, $k_2 = 14.136$, and $k_3 = 16.846$. One can easily check that all three waves with corresponding wave numbers are presented in the Fourier spectra of vibrations generated by "demon" moving with $v = 0.1$.

Critical electric field

The equations of motion (4) and (5) do not imply any limitation on value of electric field. Really, we did not find a maximum field in the range of reasonable values if appropriate initial conditions are chosen, in particular the field switching-on rate is rather low. The situation drastically changes if the field is switch on instantaneously, and it is the instantaneous field switching-on has a physical sense.

The theoretical estimation of critical field has been reported.⁸⁰ Estimations are based on the fact that, when the large field is switched on instantly, a tilted potential is formed. The heavy and slow lattice does not have time to readjust. However, the electron can tunnel through the potential.

The critical field is defined as a field, when the probability of tunneling per unit time Γ_{tun} is of the same order of magnitude as the reciprocal of the lattice readjusting time, Γ_{lat} . For analytical estimations the triangular barrier is considered. Then the tunnelling probability can be estimated by the WKB method.⁸⁴ In the case of initial standing polaron the barrier height (the electronic part of the polaron binding energy) is $e_b = \chi^4/(K^2 t_0)$ ^{80,85} and tunnelling is

$$\Gamma_{\text{tun}} = 4\exp\left[-\frac{4e_b^{3/2}}{3t_0^{1/2}eEa}\right] \quad (10)$$

The lattice readjusting time is estimated as the time necessary for the sound to pass a distance equal to the sum of the polaron width and the barrier width. Then Γ_{lat} has the form

$$\Gamma_{\text{lat}} = \frac{v_{\text{snd}}}{e_b/eEa+1/\chi^2} \quad (11)$$

The critical field can be estimated as

$$\Gamma_{\text{lat}} = \Gamma_{\text{tun}} \quad (12)$$

Since the tunnelling has a physical meaning in the continuum limit the above relations are true when the continuum approximation works, i.e. for sufficiently small χ . As we have already noted, $\chi = 0.4$ is the limiting value of the electron-phonon interaction, when the continuum approximation is well applicable. So we can expect an agreement between analytical and numerical estimations of critical field. For $\chi = 0.4$, eqns. (10)-(12) give values $E^{\text{cr}} \approx 0.00071$ in dimensionless units, which corresponds to $B^{\text{cr}} = eaE^{\text{cr}}/\hbar \approx 0.076$.

In numerical experiment we determine the fraction of electron density remaining on the polaron $\Delta|\Psi|^2$ if the field is switched on instantly in the case of initial standing polaron (see figure 8). For field upto $B \approx 0.04$, almost 100 % of electron density is localized at the polaron. For higher values of B , $\Delta|\Psi|^2$ drastically decreases. We define the critical field as a field at which about 90 % of the total electron density remains on the polaron. Then numerical experiment gives $B_{\text{cr}}^{\text{num}} \approx 0.07$, which is in good agreement with analytical estimation. This value corresponds to $4.7 \cdot 10^7$ V/m in dimension units. (Figure 8)

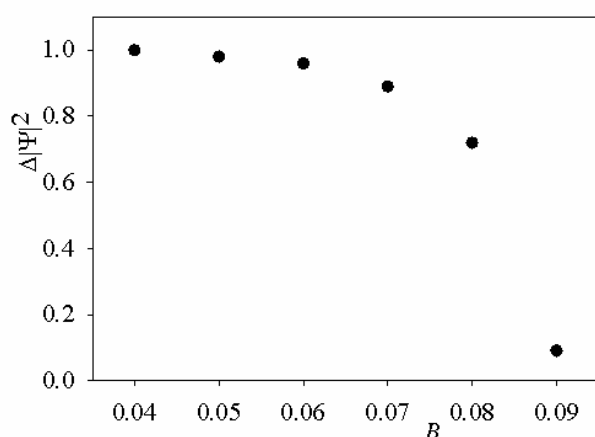


Figure 8. A fraction of electron density localized on the polaron $\Delta|\Psi|^2$ after the instantaneous switching-on of the electric field vs field parameter B ; $\chi = 0.4$.

In the case of $\chi = 1.2$, we can hardly expect such a coincidence between theoretical prediction and numerical results, because for large values of χ , the continuum

approximation does not work. However, some estimations can be done. For $\chi = 1.2$, the manually fitted parameters are $A \approx 0.78$ and $d \approx 0.7$ for standing polaron and the numerically calculated barrier height (the electronic part of the polaron coupling energy) is about 0.96. Then equations (10)-(12) give the magnitude of the critical field parameter $B_{1.2}^{\text{cr}} \approx 18$. This value is slightly higher than those estimated numerically $B_{1.2}^{\text{num}} \approx 13$. However, taking into account that equations (10)-(12) are derived in an approximation that does not work for $\chi = 1.2$, such a coincidence is surprising. Note, $B_{1.2}^{\text{num}}$ corresponds to $2 \cdot 10^8$ V/m for DNA.

CONCLUSIONS

Polarons on harmonic lattice with EPI parameter corresponding PA and DNA are very stable in a constant electric field.

The results of the numerical simulation are rather sensitive to the initial conditions and to the method of switching-on the electric field. The main criterion of the simulation correctness is the complete localization of the electron density on the polaron. With unsuccessful initial conditions, a part of the electron density decouples from the lattice deformation. In all presented results at least 99 % of the total electron density is localized on the polaron. In the case of complete localization of the electron density on the polaron, the results do not depend on the initial conditions and the method of switching-on the electric field.

The polaron moves with constant velocity in electric field. The dependence of the stationary velocity on the applied field is weakly logarithmic. Within four orders of magnitude of the field strength, stationary velocities vary ≤ 10 %. This means that in polyacetylene and DNA the dependence of the polaron velocity on the applied electric field is insignificant.

The parameters (amplitude, width, velocity) of a stationary moving polaron in an electric field coincide with the parameters of a polaron moving with the same velocity in the absence of an electric field, which indicates the adiabatic polaron movement.

Polaron moving in electric field generates coherent oscillations. The spectral characteristics of the generated oscillation are well described by a simple "demon" model. This means that any moving localized excitation of arbitrary shape generates coherent oscillations of the harmonic lattice. The phase velocity of generated oscillations is equal to the polaron/"demon" velocity.

For appropriate initial conditions, i.e. adiabatically slow field switching-on rate or initially moving polaron, we did not find maximum value of the electric field resulting in polaron destruction. However, in the case of instantaneous field switching-on, rather low fields destroy initially standing polaron. The estimated values of critical field are $4.7 \cdot 10^7$ V m⁻¹ and $2 \cdot 10^8$ Vm⁻¹ for polyacetylene and DNA, respectively.

The numerical results of present work are in good agreement with theoretical predictions reported earlier.⁸⁰

References

- ¹Friedman, K. A., Heller, A., On the Non-Uniform Distribution of Guanine in Introns of Human Genes: Possible Protection of Exons against Oxidation by Proximal Intron Poly-G Sequences, *J. Phys. Chem. B*, **2001**, *105*, 11859. DOI: 10.1021/jp012043n
- ²Endres, R. G., Cox D. L., Singh R. R. P., The quest for high-conductance DNA, *Rev. Mod. Phys.*, **2004**, *76*, 195. DOI: 10.1103/RevModPhys.76.195
- ³Fink, H.-W., Schonenberger, Ch., Electrical conduction through DNA molecules, *Nature*, **1999**, *398*, 407. DOI:10.1038/18855
- ⁴Porath, D., Bezryadin, A., de Vries, S., Dekker, C., Direct measurement of electrical transport through DNA molecules, *Nature*, **2000**, *403*, 635. DOI:10.1038/35001029
- ⁵Genereux, J. C., Barton, J. K., Mechanisms for DNA Charge Transport, *Chem. Rev.*, **2010**, *110*, 1642. DOI: 10.1021/cr900228f
- ⁶Genereux, J. C., Wuerth, S. M., Barton, J. K., Single-Step Charge Transport through DNA over Long Distances., *J. Am. Chem. Soc.*, **2011**, *133*, 3863. DOI: 10.1021/ja107033v
- ⁷Arikuma, Y., Nakayama, H., Morita, T., Kimura, S., Electron Hopping over 100 Å Along an α Helix, *Angew. Chem. Int. Ed.*, **2010**, *49*, 1800. DOI: 10.1002/anie.200905621
- ⁸Augustyn, K. E., Genereux, J. C., Barton, J. K., Distance-Independent DNA Charge Transport across an Adenine Tract, *Angew. Chem. Int. Ed.*, **2007**, *46*, 5731. DOI: 10.1002/anie.200701522
- ⁹Barton J. K., Olmon E. D., Sontz, P. A., Metal Complexes for DNA-Mediated Charge Transport, *Coordin. Chem. Rev.*, **2011**, *255*, 619. DOI: 10.1016/j.ccr.2010.09.002
- ¹⁰Slinker, J. D., Muren, N. B., Renfrew, S. E., Barton, J. K., DNA charge transport over 34 nm, *Nat. Chem.*, **2011**, *3*, 228. DOI:10.1038/nchem.982
- ¹¹Cordes, M., Giese, B., Electron transfer in peptides and proteins, *Chem. Soc. Rev.*, **2009**, *38*, 892. DOI: 10.1039/B805743P
- ¹²Astakhova, T. Yu., Likhachev, V. N., Vinogradov, G. A., Long-range charge transfer in biopolymers, *Russ. Chem. Rev.*, **2012**, *81*, 994. DOI: 10.1070/RC2012v081n11ABEH004308
- ¹³Su, W. P., Schrieffer, J. R., Heeger, A. J., Solitons in Polyacetylene, *Phys. Rev. Lett.*, **1979**, *42*, 1698. DOI: 10.1103/PhysRevLett.42.1698
- ¹⁴Su, W. P., Schrieffer, J. R., Heeger, A. J., Soliton excitations in polyacetylene, *Phys. Rev. B*, **1980**, *22*, 2099. DOI: 10.1103/PhysRevB.22.2099
- ¹⁵Su, W. P., Schrieffer, J. R., Soliton dynamics in polyacetylene, *Proc. Natl. Acad. Sci. USA*, **1980**, *77*, 5626. DOI: 10.1073/pnas.77.10.5626
- ¹⁶Su, W. P., Schrieffer, J. R., Fractionally Charged Excitations in Charge-Density-Wave Systems with Commensurability 3, *Phys. Rev. Lett.*, **1981**, *46*, 738. DOI: 10.1103/PhysRevLett.46.738
- ¹⁷Takayama, H., Lin-Liu, Y. R., Maki K., Continuum model for solitons in polyacetylene, *Phys. Rev. B*, **1980**, *21*, 2388. DOI: 10.1103/PhysRevB.21.2388
- ¹⁸Wilson, E. G., *J. Phys. C*, A new theory of acoustic solitary-wave polaron motion, **1983**, *16*, 6739. DOI: 10.1088/0022-3719/16/35/008
- ¹⁹Arikabe Y., Kuwabara, M., Ono, Y., Dynamics of an Acoustic Polaron in One-Dimensional Electron-Lattice System, *J. Phys. Soc. Jpn.*, **1996**, *65*, 1317. DOI: 10.1143/jpsj.65.1317
- ²⁰Marcus, R. A., Electron Transfer Reactions in Chemistry: Theory and Experiment, *Angew. Chem., Int. Edit.*, **1993**, *32*, 1111. DOI: 10.1002/anie.199311113
- ²¹Sartor, V., Boone, E., Schuster, G. B., Long-Distance Radical Cation Migration through A/T Base Pairs in DNA: An Experimental Test of Theory, *J. Phys. Chem. B*, **2001**, *105*, 11057. DOI: 10.1021/jp011354v
- ²²Meggers, E., Michel-Beyerle, M. E., Giese, B., Sequence Dependent Long Range Hole Transport in DNA, *J. Am. Chem. Soc.*, **1998**, *120*, 12950. DOI: 10.1021/ja983092p
- ²³Conwell, E. M., Rakhmanova, S. V., Polarons in DNA, *Proc. Natl. Acad. Sci. USA*, **2000**, *97*, 4556. DOI: 10.1073/pnas.050074497
- ²⁴Rakhmanova, S. V., Conwell, E. M., Polaron Motion in DNA, *J. Phys. Chem. B*, **2001**, *105*, 2056. DOI: 10.1021/jp0036285
- ²⁵Conwell, E. M., Basko, D. M., Hole Traps in DNA, *J. Am. Chem. Soc.*, **2001**, *123*, 11441. DOI: 10.1021/ja015947v
- ²⁶Conwell, E. M., Charge transport in DNA in solution: The role of polarons, *Proc. Natl. Acad. Sci.*, **2005**, *102*, 8795. DOI: 10.1073/pnas.0501406102
- ²⁷Komineas, S., Kalosakas, G., Bishop, A. R., Effects of intrinsic base-pair fluctuations on charge transport in DNA, *Phys. Rev. E*, **2002**, *65*, 061905. DOI: 10.1103/PhysRevE.65.061905
- ²⁸Kalosakas, G., Rasmussen, K. O., Bishop, A. R., Charge trapping in DNA due to intrinsic vibrational hot spots, *J. Chem. Phys.*, **2003**, *118*, 3731. DOI: 10.1063/1.1539091
- ²⁹Chang, C.-M., Castro Neto, A. H., Bishop, A.R., Long-range charge transfer in periodic DNA through polaron diffusion, *Chem. Phys.*, **2004**, *303*, 189. DOI: 10.1016/j.chemphys.2004.05.015
- ³⁰Berashevich, J. A., Bookatz, A. D., Chakraborty, T., The electric field effect and conduction in the Peyrard–Bishop–Holstein model, *J. Phys.- Condens. Mat.*, **2008**, *20*, 035207. DOI: 10.1088/0953-8984/20/03/035207
- ³¹Berashevich, J. A., Chakraborty, T., Electronic parameters for the hole transfer in DNA duplex oligomers, *Chem. Phys. Lett.*, **2007**, *446*, 159. DOI: 10.1016/j.cplett.2007.08.045
- ³²Hawke, L. G. D., Kalosakas, G., Simserides, C., Electronic parameters for charge transfer along DNA, *Eur. Phys. J. E*, **2010**, *32*, 291. DOI: 10.1140/epje/i2010-10650-y
- ³³Yamada, H., Starikov, E. B., Hennig, D., Quantum diffusion in polaron model of poly(dG)-poly(dC) and poly(dA)-poly(dT) DNA polymers, *Eur. Phys. J. B*, **2007**, *59*, 185. DOI: 10.1140/epjb/e2007-00274-4
- ³⁴Kalosakas, G., Charge transport in DNA: Dependence of diffusion coefficient on temperature and electron-phonon coupling constant, *Phys. Rev. E*, **2011**, *84*, 051905. DOI: 10.1103/PhysRevE.84.051905
- ³⁵Kucherov, V. M., Kinz-Thompson, C. D., Conwell, E. M., Polarons in DNA Oligomers, *J. Phys. Chem. C*, **2010**, *114*, 1663. DOI: 10.1021/jp908809t
- ³⁶Qu Z., Kang, D. W., Jiang, H., Xie, S. J., Temperature effect on polaron dynamics in DNA molecule: The role of electron-base interaction, *Physica B*, **2010**, *405*, S123. DOI: 10.1016/j.physb.2009.12.020
- ³⁷Triberis, G., Simserides, C., Karavolas, V., A small polaron hopping model for multiphonon-assisted transport along DNA molecules, in the presence of disorder, *Physica E*, **2006**, *32*, 592. DOI: 10.1016/j.physe.2005.12.111
- ³⁸Cuniberti, G., Fagas, G., Richter, K., Fingerprints of mesoscopic leads in the conductance of a molecular wire, *Chem. Phys.*, **2002**, *281(2-3)*, 465. DOI: 10.1016/S0301-0104(02)00341-5
- ³⁹Todorov, T. N., Tight-binding simulation of current-carrying nanostructures, *J. Phys.-Condens. Mat.*, **2002**, *14(11)*, 3049. DOI: 10.1088/0953-8984/14/11/314
- ⁴⁰Lima, M. P., e Silva, G. M., Dynamical evolution of polaron to bipolaron in conjugated polymers, *Phys. Rev. B*, **2006**, *74*, 224304. DOI: 10.1103/PhysRevB.74.224304

- ⁴¹e Silva, G. M., Electric-field effects on the competition between polarons and bipolarons in conjugated polymers, *Phys. Rev. B*, **2000**, *61*, 10777. DOI: 10.1103/PhysRevB.61.10777
- ⁴²Peng, C., Jian, W., GuiQing, Zh., ChengBu, L., Hole polarons in poly(G)-poly(C) and poly(A)-poly(T) DNA molecules, *Sci. China Ser. B*, **2008**, *51*, 1182. DOI: 10.1007/s11426-008-0128-y
- ⁴³Basko, D. M., Conwell, E. M., Self-trapping versus trapping: Application to hole transport in DNA, *Phys. Rev. E*, **2002**, *65*, 061902. DOI: 10.1103/PhysRevE.65.061902
- ⁴⁴Zheng, B., Wu, J., Sun, W., Liu, Ch., Trapping and hopping of polaron in DNA periodic stack, *Chem. Phys. Lett*, **2006**, *425*, 123. DOI:10.1016/j.cplett.2006.05.022
- ⁴⁵Lin, X., Li, J., Smela, E., Yip, S., Polaron-induced conformation change in single polypyrrole chain: An intrinsic actuation mechanism, *Int. J. Quantum Chem.*, **2005**, *102*, 980. DOI: 10.1002/qua.20433
- ⁴⁶Falleiros, M. B., e Silva, G. M., Polaron and bipolaron stability on paraphenylene polymers, *J. Mol. Model.*, **2017**, *23*, 59. DOI: 10.1007/s00894-017-3215-1
- ⁴⁷Ma, H., Schollwock, U., Dynamical simulations of polaron transport in conjugated polymers with the inclusion of electron-electron interactions, *J. Phys. Chem. A*, **2009**, *113*(7), 1360. DOI: 10.1021/jp809045r
- ⁴⁸Ribeiro, L. A., da Cunha, W. F., de O. Neto, P. H., Gargano, R., e Silva, G. M., Effects of temperature and electric field induced phase transitions on the dynamics of polarons and bipolarons, *New J. Chem.*, **2013**, *37*, 2829. DOI: 10.1039/c3nj00602f
- ⁴⁹Hultell, M., Stafstrom, S., Polaron dynamics in highly ordered molecular crystals, *Chem. Phys. Lett.*, **2006**, *428*, 446. DOI:10.1016/j.cplett.2006.07.042
- ⁵⁰Johansson, A., Stafstrom, S., Polaron Dynamics in a System of Coupled Conjugated Polymer Chains, *Phys. Rev. Lett.*, **2001**, *86*, 3602. DOI: 10.1103/PhysRevLett.86.3602
- ⁵¹Johansson, A., Stafstrom, S., Soliton and polaron transport in *trans*-polyacetylene, *Phys. Rev. B*, **2002**, *65*, 045207. DOI: 10.1103/PhysRevB.65.045207
- ⁵²Alexandrov, A. S., Yavidov, B. Ya., Small adiabatic polaron with a long-range electron-phonon interaction, *Phys. Rev. B*, **2004**, *69*, 073101. DOI: 10.1103/PhysRevB.69.073101
- ⁵³Diaz, E., Lima, R. P. A., Dominguez-Adame, F., Bloch-like oscillations in the Peyrard-Bishop-Holstein model, *Phys. Rev. B*, **2008**, *78*, 134303. DOI: 10.1103/PhysRevB.78.134303
- ⁵⁴Hague, J. P., Kornilovitch, P. E., Alexandrov, A. S., Samson, J. H., Effects of lattice geometry and interaction range on polaron dynamics, *Phys. Rev. B*, **2006**, *73*, 054303. DOI: 10.1103/PhysRevB.73.054303
- ⁵⁵Mozafari, E., Stafstrom, S., Polaron dynamics in a two-dimensional Holstein-Peierls system, *J. Chem. Phys.*, **2013**, *138*, 184104. DOI: 10.1063/1.4803691
- ⁵⁶Wei, J. H., Liu, X. J., Berakdar, J., Yan, YiJing, Pathways of polaron and bipolaron transport in DNA double strands, *J. Chem. Phys.*, **2008**, *128*, 165101. DOI: 10.1063/1.2902279
- ⁵⁷Luo, J., Piette, B. M. A. G., A generalised Davydov-Scott model for polarons in linear peptide chains, *Eur. Phys. J. B*, **2017**, *90*, 155. DOI: 10.1140/epjb/e2017-80209-2
- ⁵⁸Hennig, D., Neibner, C., Velarde, M. G., Ebeling, W., Effect of anharmonicity on charge transport in hydrogen-bonded systems, *Phys. Rev. B*, **2006**, *73*, 024306. DOI: 10.1103/PhysRevB.73.024306
- ⁵⁹da Cunha, W. F., Neto, P. H. de O., Gargano, R., e Silva, G. M., Temperature effects on polaron stability in polyacetylene, *Int. J. Quantum Chem.*, **2008**, *108*, 2448. DOI: 10.1002/qua.21798
- ⁶⁰Zhang, Y. L., Liu, X. J., An, Z., Temperature dependence of polaron stability in conjugated polymers, *Europhys. Lett*, **2015**, *111*, 17009. DOI: 10.1209/0295-5075/111/17009
- ⁶¹Yao, Y., Qiu, Y., Wu, Ch.-Q., Dissipative dynamics of charged polarons in organic molecules, *J. Phys.- Condens. Matter*, **2011**, *23*, 305401. DOI: 10.1088/0953-8984/23/30/305401
- ⁶²Ojeda J. H., Lima, R. P. A., Dominguez-Adame, F., Orellana, P. A., Trapping and motion of polarons in weakly disordered DNA molecules, *J. Phys.- Condens. Matter*, **2009**, *21*, 285105. DOI:10.1088/0953-8984/21/28/285105
- ⁶³Zhang, G., Cui, P., Wu, J., Liu, Ch., Structural fluctuation effect on the polaron in DNA, *Physica B*, **2009**, *404*, 1485. DOI:10.1016/j.physb.2009.01.004
- ⁶⁴Yan, Y. H., An, Z., Wu, C.Q., Dynamics of polaron in a polymer chain with impurities, *Eur. Phys. J. B*, **2004**, *42*, 157. DOI: 10.1140/epjb/e2004-00367-6
- ⁶⁵Wang, Y. D., Zhang, X. G., Meng, Y., Di, B., Zhang, Y. L., An, Z., Dynamic recombination of polaron pair with impurity in conjugated polymers, *Org. Electron.*, **2017**, *49*, 286. DOI: 10.1016/j.orgel.2017.06.067
- ⁶⁶Johansson, A., Stafstrom, S., Nonadiabatic simulations of polaron dynamics, *Phys. Rev. B*, **2004**, *69*, 235205. DOI: 10.1103/PhysRevB.69.235205
- ⁶⁷Li, Y., Liu, X.-J., Fu, J.-Y., Liu, D.-Sh., Xie, Sh.-J., Mei, L.-M., Bloch oscillations in a one-dimensional organic lattice, *Phys. Rev. B*, **2006**, *74*, 184303. DOI: 10.1103/PhysRevB.74.184303
- ⁶⁸Ono, Y., Terai, A., Motion of Charged Soliton in Polyacetylene Due to Electric Field, *J. Phys. Soc. Jpn.*, **1990**, *59*, 2893. DOI: 10.1143/JPSJ.59.2893
- ⁶⁹Liu, X., Gao, K., Fu, J., Li, Y., Wei, J., Xie, Sh., Effect of the electric field mode on the dynamic process of a polaron, *Phys. Rev. B*, **2006**, *74*, 172301. DOI: 10.1103/PhysRevB.74.172301
- ⁷⁰Zhang, G., Hu, H., Cui, S., Lv, Z., Higher order tight binding Su-Schrieffer-Heeger method and its applications in DNA charge transport, *Physica B*, **2010**, *405*, 4382. DOI:10.1016/j.physb.2010.07.047
- ⁷¹Thornber, K. K., Feynman, R. P., Velocity Acquired by an Electron in a Finite Electric Field in a Polar Crystal, *Phys. Rev. B*, **1970**, *1*, 4099. DOI: 10.1103/PhysRevB.1.4099
- ⁷²Ribeiro, L. A., da Cunha, W. F., Fonseca, A. L. de A., e Silva, G. M., Bloch oscillations in organic and inorganic polymers, *J. Chem. Phys.*, **2017**, *146*, 144903. DOI: 10.1063/1.4979950
- ⁷³da Silva, M. V. A., Neto, P. H. de O., Cunha, W. F. da, Gargano, R., e Silva, G. M., Supersonic quasi-particles dynamics in organic semiconductors, *Chem. Phys. Lett.*, **2012**, *550*, 146. DOI: 10.1016/j.cplett.2012.09.012
- ⁷⁴Rakhmanova, S. V., Conwell, E. M., Polaron dissociation in conducting polymers by high electric fields, *Appl. Phys. Lett.*, **1999**, *75*, 1518. DOI: 10.1063/1.124741
- ⁷⁵Rakhmanova, S. V., Conwell, E. M., Nonlinear dynamics of an added carrier in *trans*-polyacetylene in the presence of an electric field, *Synthetic Met.*, **2000**, *110*, 37. DOI: 10.1016/S0379-6779(99)00261-1
- ⁷⁶Mahani, M. R., Mirsakiyeva, A., Delin, A., Breakdown of Polarons in Conducting Polymers at Device Field Strengths, *Phys. Chem. C*, **2017**, *121*, 10317. DOI: 10.1021/acs.jpcc.7b02368
- ⁷⁷Yu, J. F., Wu, C. Q., Sun, X., Nasu, K., Breather in the motion of a polaron in an electric field, *Phys. Rev. B*, **2004**, *70*, 064303. DOI: 10.1103/PhysRevB.70.064303
- ⁷⁸Vidmar, L., Bonca, J., Mierzejewski, M., Prelovsek, P., Trugman, S. A., Nonequilibrium dynamics of the Holstein polaron driven by an external electric field, *Phys. Rev. B*, **2011**, *83*, 134301. DOI: 10.1103/PhysRevB.83.134301

- ⁷⁹Nazareno, H. N., de Brito, P. E., Bloch oscillations as generators of polarons in a 1D crystal, *Physica B*, **2016**, 494, 1. DOI: 10.1016/j.physb.2016.04.029
- ⁸⁰Basko, D. M., Conwell, E. M., Stationary Polaron Motion in a Polymer Chain at High Electric Fields, *Phys. Rev. Lett.*, **2002**, 88, 056401. DOI: 10.1103/PhysRevLett.88.056401
- ⁸¹Likhachev, V. N., Astakhova, T. Yu., Vinogradov G.A., Поляроны в одномерной решетке. I. Неподвижный полярон *Russ. Khim. Fiz.*, **2013**, 32, 3. DOI: 10.7868/S0207401X13040092
- ⁸²Carstea, A. S., Integrable systems related to Su-Schrieffer-Heeger lattices, *Chaos Soliton Fract*, **2009**, 42, 923. DOI: 10.1016/j.chaos.2009.02.034
- ⁸³Astakhova, T. Yu., Likhachev, V. N., Vinogradov, G. A., Polaron on a one-dimensional lattice: II. A moving polaron, *Russ. J. Phys. Chem. B*, **2013**, 7, 521. DOI: 10.1134/S199079311305028X
- ⁸⁴Landau, L. D., Lifshitz, E. M., *Quantum Mechanics, Non-relativistic Theory, Second edition, revised and enlarged*, Pergamon Press, **1965**, 174-175.
- ⁸⁵Landau, L. D., Lifshitz, E.M., *Quantum Mechanics, Non-relativistic Theory, Second edition, revised and enlarged*, Pergamon Press, **1965**, 72-73.

Received: 01.06.2018.

Accepted: 17.08.2018.